

Modal Bandwidth Enhancement in a Plastic Optical Fiber by W-Refractive Index Profile

Takaaki Ishigure, *Member, IEEE*, Hideki Endo, Kunihiro Ohdoko, Keita Takahashi, and Yasuhiro Koike, *Member, IEEE*

Abstract—A plastic optical fiber (POF) having a W-shaped refractive index profile (W-shaped POF) was prepared for the first time that had a possibility to realize a higher bit rate transmission than those of the conventional silica-based multimode fiber and graded index (GI) POF links. Since the W-shaped POF has a valley of the refractive index at the boundary of the core and cladding of the conventional graded-index (GI) POF, the group delay of higher order modes is strongly influenced, and the modal dispersion in the GI POF is compensated. By comparing the propagating mode properties of the W-shaped POF with those of the GI POF, we clarified theoretically and experimentally that the index valley has a remarkable modal dispersion compensation effect.

Index Terms—Modal dispersion, mode-coupling, differential mode attenuation, plastic optical fiber (POF), W-shaped index profile.

I. INTRODUCTION

THE data communications market has risen to the forefront in lightwave communications in the past five years, because of the increasing need for higher bandwidth. Silica-based optical fiber networks are widely utilized in the long-haul telecommunications field and currently even in metropolitan area networks. In addition to such applications, the required data rate in the local area network (LAN) becomes 10 Gb, where optical fiber links are playing major roles to cover such a high data rate. However, in the case of silica-based single-mode fibers, the core diameter is approximately 10 μm , which requires accurate alignment in optical couplings and fiber connections. For this reason, a resurgence of interest in multimode fibers (MMFs) has accomplished the proposal for gigabit and 10 Gb Ethernet MMF-based physical media dependent (PMD). For MMF links, inexpensive vertical cavity surface emitting laser (VCSEL)-based transceivers should be adopted to offer low cost optical networks. Therefore, it would not necessarily be the best solution to distribute such silica-based single-mode optical fibers even to office and home networks because of the cost of fiber optic devices such as connectors and transceivers.

On the other hand, a plastic optical fiber (POF), having a much larger core than silica fibers, is expected to be the office and home network medium because its large core and great

mechanical flexibility allow an easy network installation. We have proposed a high-bandwidth graded-index (GI) POF [1], [2] that has a quadratic refractive index profile in the core region, and have improved its bandwidth characteristics. In this paper, a remarkable refractive index profile that includes an index valley at the core cladding boundary (the index profile becomes W-shaped) is proposed to maximize its modal bandwidth. The W-shaped index profile is widely utilized in a dispersion shifted single mode silica fiber. Formation of the W-shaped index profile in a silica-based MMF was proposed by Okoshi, Oyamada, and Okamoto [3], [4] about 30 years ago to decrease the modal dispersion in GI fibers. They showed only theoretically that an index valley in the W-shaped index profile lowered the modal dispersion compared to the GI fiber with an ideal index profile, where only small number of modes (~ 20) were assumed to be supported by the MMF. However, there are few reports on the preparation and characterization of W-shaped MMFs, while several are for accurate index profiling of silica-based GI MMFs [5]. In this paper, the advantage of the W-shaped index profile in the bandwidth was verified both theoretically and experimentally in a large core POF that supported a large number of modes.

For achieving the high bit rate transmission even by the legacy MMFs, a restricted launch condition is proposed and mainly utilized [6], [7]. Actually, this under-filled launch (UFL) condition enables the silica-based MMF to transmit at 10 Gb/s data rate for 300 m [8]. The UFL condition can be, of course, applied to the large core GI POF. However, the UFL condition that is achieved by a small spot of light beam from the laser and/or VCSEL sources on the input fiber end needs a precise alignment between the light source and fiber. However, adopting the same launch technology to POF takes few advantages of its large core. The GI POF with a large core has possibilities to tolerate such coupling alignment accuracy, if it can maintain a high-bandwidth performance independent of the launch condition. Therefore, high-bandwidth under over-filled launch condition (OFL,) which has been achieved by the accurate index profiling so far, has several advantages. Particularly, we have developed the perfluorinated polymer-based GI POF (PF GI POF) that has extremely low material dispersion. It was already clarified that [9] the PF GI POF that has the material dispersion lower even than silica, enabled the PF GI POF to potentially exhibit higher bandwidth than silica-based MMFs. Furthermore, such a high-bandwidth GI POF can be applied to the optical interconnection combined with VCSEL arrays. For such new dimensions of POF, in this paper, the high-bandwidth performance even under OFL is considered for large core POF.

Manuscript received May 18, 2004; revised November 4, 2004.

T. Ishigure, K. Ohdoko, K. Takahashi, and Y. Koike are with Faculty of Science and Technology, Keio University, Yokohama 223-8522, Japan, and Japan Science and Technology Agency (JST) ERATO, Kawasaki, Japan (e-mail: ishigure@appi.keio.ac.jp).

H. Endo is with Central Research Laboratory, Hitachi Ltd., Musashino 185-860, Japan.

Digital Object Identifier 10.1109/JLT.2005.844203

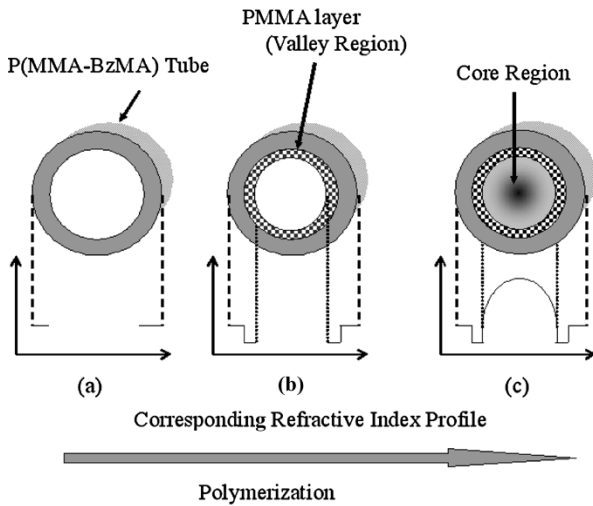


Fig. 1. Schematic representation of the formation process of a W-shaped refractive index profile in a plastic preform rod.

II. EXPERIMENTAL

A. Fiber Preparation

The W-shaped POE was obtained by the heat-drawing of a preform, in which the W-shaped index profile was already formed. The fiber diameter was 0.75 mm. A schematic representation of the process to form the W-shaped refractive index profile is shown in Fig. 1. At first, a copolymer tube of methyl methacrylate (MMA) and benzyl methacrylate (BzMA) (=9 : 1 by weight) was prepared from the purified monomers. After polymerizing the P(MMA-BzMA) tube, [see Fig. 1(a)] a specified amount of MMA monomer was injected into the tube, and the tube was rotated on its axis at 3000 rpm in an oven at 70 °C to polymerize the PMMA homopolymer layer. After the polymerization, the tube having the index valley as shown in Fig. 1(b) was obtained, because the refractive index ($n_d = 1.498$) of P(MMA-BzMA) copolymer is slightly higher than that ($n_d = 1.492$) of PMMA layer. Subsequently, the tube was filled with the MMA monomer-dopant (diphenyl sulfide) mixture to form the quadratic refractive index profile in the core region [see Fig. 1(c)], [10]. The formation mechanism of the quadratic refractive index profile in the core by the interfacial-gel polymerization process [see Fig. 1(c)] is described in [2] and [11].

B. Refractive Index Profile

It is well known that the modal dispersion of an MMF is decreased by a quadratic refractive index profile. We already reported that the refractive index profile of the GI POE could be widely controlled by the interfacial-gel polymerization process [11], [12], and succeeded in obtaining an optimum refractive index profile in a PMMA-based POE. Fig. 2 shows the experimentally measured refractive index profile of the W-shaped POE (solid line) compared with the conventional GI POE (broken line). For a quantitative analysis of the bandwidth, the refractive index profile was approximated by a power-law equation shown by (1), [13]

$$\begin{aligned} n(r) &= n_1 \left[1 - 2\rho\Delta \left(\frac{r}{a} \right)^g \right]^{1/2} & 0 \leq r \leq a \\ &= n_2 & r \geq a \end{aligned} \quad (1)$$

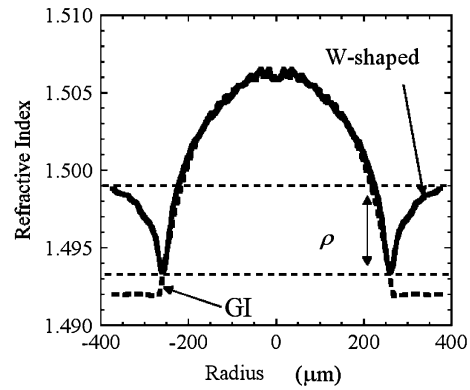


Fig. 2. Comparison of the refractive index profiles between the W-shaped POE (solid line) and the GI POE (broken line). These two POEs have the same index exponent ($g = 2.9$) in the core index profile.

where n_1 and n_2 are the refractive indices of the core center and cladding, respectively, a is the core radius, and Δ is the relative index difference defined as

$$\Delta = \frac{n_1^2 - n_2^2}{2n_1^2}. \quad (2)$$

The parameter g , called the index exponent, determines the refractive index profile. The new parameter ρ in (1) signifies the depth of the index valley as shown in Fig. 2. When ρ equals 1, the profile is the same as the conventional quadratic refractive index profile followed by the uniform index cladding (GI type), while the W-shaped index profile has the parameter ρ larger than 1.

The refractive index profiles of both W-shaped and GI POEs agree in the core region (except for the index valley) as shown in Fig. 2, and they are well fitted to the power-law form [see (1)] with $g = 2.9$. In the W-shaped POE, the approximated ρ value was 1.7. By comparing the bandwidth performances of these two fibers, the modal dispersion compensation effect of the index valley was experimentally confirmed.

III. RESULTS AND DISCUSSION

A. Comparison of Bandwidths

The bandwidth measurement results of two POEs at a 0.65- μm wavelength are shown in Fig. 3. The bandwidth measurement was performed by a well known time-domain measurement method where an overfilled launch (OFL) condition [14] was adopted to confirm the effect of the refractive index profile in the whole core region on the group delay of all the modes. It is a current trend that the OFL condition is not necessarily a suitable launch condition for an MMF when an application to a short-reach, high-speed network is considered [14]. However, since this paper simply aims to show the advantage of the W-shaped index profile compared to the conventional GI, the OFL condition was adopted [15], [16]. In Fig. 3, the output pulse width from the W-shaped POE is narrower than that from the GI POE, despite the same index profile in the quadratic part of the core region as shown in Fig. 2. Estimated -3 dB bandwidth of the W-shaped POE obtained by Fourier transform of the output pulse results was 1.5 GHz for 100-m, which is approximately 1.5 times higher than that

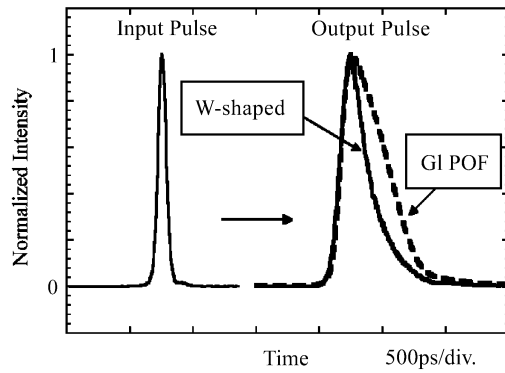


Fig. 3. The bandwidth performance measurement results of 100-m W-shaped (solid line) and GI (broken line) POFs at 0.65- μm wavelength. Estimated -3 dB bandwidths by Fourier Transform; W-shaped 1.5 GHz; GI: 1.1 GHz.

(1.1 GHz for 100-m) of the GI POF. The difference observed in the bandwidth performances in these two POFs is analyzed in detail in the next sections. Since both POFs shown in Fig. 3 were formed basically with PMMA, the measured bandwidths are much lower than that required for 10 Gbps transmission because of the large material dispersion of PMMA in addition to the modal dispersion [17]. However, as the main purpose of this paper is in the comparison of modal dispersion between the GI and W-shaped POFs, the results of PMMA-based fibers shown in Fig. 3 are considered to be sufficient. The advantage in the low modal dispersion of W-shaped profile can be applied to the PF polymer-based POF with low-loss and low-material dispersion [9], by which extremely high bandwidth performance is expected.

B. Propagating Mode Characteristics

Several factors by which the bandwidth performance of an MMF is improved have been proposed. For instance, in the case of the POF, a mode coupling and/or differential mode attenuation (DMA) have been considered [15], [18] to be the origins of such an unexpected bandwidth increase. We also clarified that the DMA in the GI POFs strongly affected their bandwidth performances rather than mode coupling [15]. Therefore, in the case of the W-shaped POF shown in Fig. 3, the existence of both DMA and mode coupling is a concern.

In order to clarify the effect of mode coupling, the launch condition dependence of the near-field patterns (NFPs) at the output end of both GI and W-shaped POFs were measured. For exciting a restricted mode group in the POFs, a 1-m single-mode silica fiber was used as a probe fiber [15], [19]. This single-mode fiber satisfies the single-mode condition at 0.65- μm wavelength. Similar to the measurement of the differential mode delay (DMD), the light from a laser diode at 0.65- μm wavelength was introduced into the probe fiber. Then, the modes in POFs were selectively excited by scanning a single mode fiber across the input end-face of POFs. The NFP of the individual mode group was measured by a CCD camera [15].

The results of the 100-m W-shaped POFs whose bandwidth performance is shown in Fig. 3 are shown in Fig. 4. For a comparison, those of the GI POF are shown in Fig. 5. In both POFs, the observed spot sizes of the low-order modes are much smaller

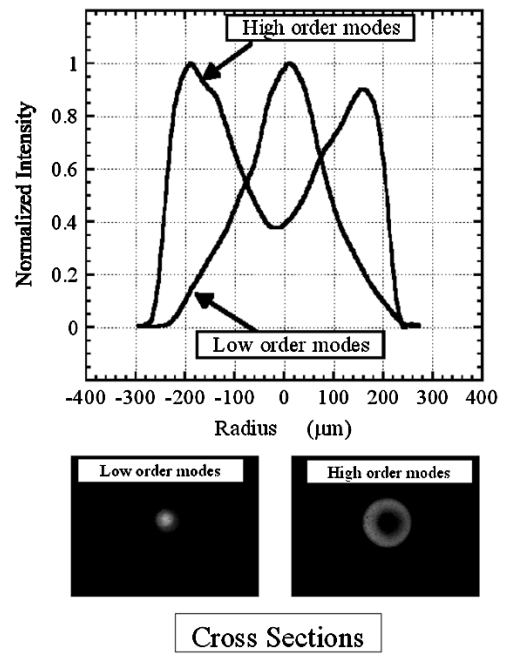


Fig. 4. Comparison of the NFPs of low-order and high-order mode groups in the W-shaped POF after 100-m transmission. Photograph: Observed patterns of the cross sections.

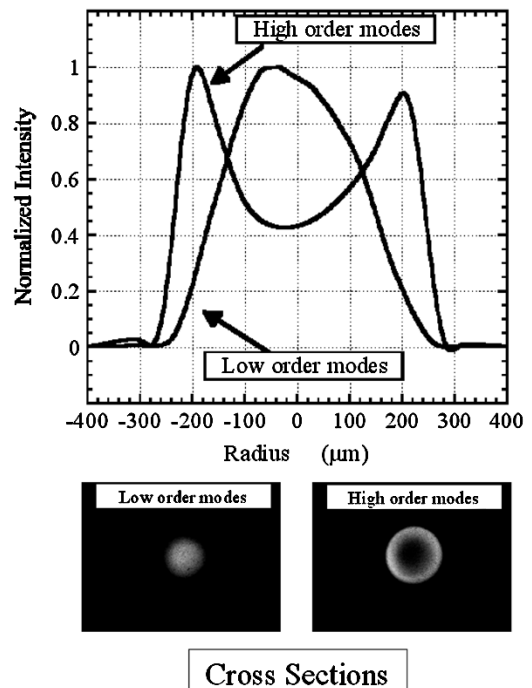


Fig. 5. Comparison of the NFPs of low-order and high-order mode groups in the GI POF after 100-m transmission. Photograph: Observed patterns of the cross sections.

than their core diameters ($\sim 500 \mu\text{m}$), which means that the electric fields of the low-order modes are well confined in the center region of the core. On the other hand, explicit ring patterns are observed in the NFPs of high-order modes in both fibers. This ring pattern is a typical NFP of the high-order modes in a GI POF [15], [18]. On the contrary, the NFP examples from the GI POF in which strong mode coupling exists are shown in Fig. 6 as a comparison. Because of the strong mode coupling, the NFP

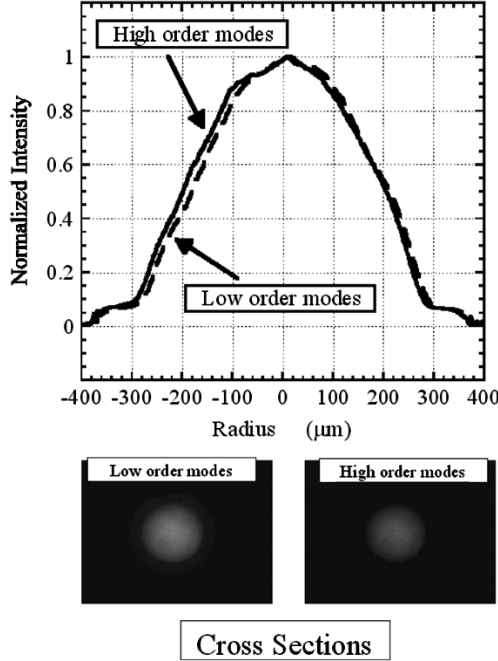


Fig. 6. Comparison of the NFPs of low-order and high-order mode groups in the GI POF having strong mode coupling after 100-m transmission. Photograph: Observed patterns of the cross sections.

showed no launch condition dependence. In such a fiber with strong mode coupling, the group delay averaged, and bandwidth performance is improved [20].

However, the remarkable differences in the NFPs between low and high-order modes observed in both GI and W-shaped POFs shown in Figs. 4 and 5 indicate that each mode is transmitted with little energy transfer among the other modes. Thus, in these two POFs, little mode coupling exists. Therefore, it was confirmed that the bandwidth improvement in the W-shaped POF compared with the GI POF was not caused by mode coupling.

C. Theoretical Estimation of Bandwidth Performance

The origin of the bandwidth improvement in the W-shaped POF was theoretically analyzed. The output pulse waveforms from the GI and W-shaped POFs were simulated from the measured refractive index profiles. The bandwidths of these POFs were theoretically calculated by approximating their index profiles by (3), which requires a numerical computation procedure for the group delay calculation. In this paper, the WKB method [15], [21] was adopted.

$$n(r) = n_1 \left[1 - 2 \cdot \Delta \cdot \sum_{m=1}^{10} \left\{ A_m \cdot \left(\frac{r}{a} \right)^m \right\} \right]^{\frac{1}{2}} \quad (3)$$

where, A_m ($m = 1, 2, \dots, 10$) is a constant independent of the wavelength of transmitted light.

In the approximation process of the refractive index profile, it was hard to accurately fit the measured profile to the approximation by (3) if a cladding with uniform refractive index and an index valley at the core-cladding boundary were included. Furthermore, in the conventional WKB numerical computation process, taking into account the cladding with

uniform refractive index and/or index valley effects makes the calculation process complicated and time consuming. In addition, calculated data by such a complicated process cannot necessarily predict the experimental data precisely. Therefore, in the calculation process of the modal dispersion in this paper, only the quadratic part of the index profile in the core region was taken into account.

The group delay τ of the mode having the propagation constant β can be expressed as [21]

$$\tau = \frac{L}{c} \frac{k}{\beta} \left\{ \left[\int_{r_1}^{r_2} \frac{n^2 + nk \frac{dn}{dk}}{R} dr \right] / \left[\int_{r_1}^{r_2} \frac{dr}{R} \right] \right\} \quad (4)$$

where n , c , and L signify the refractive index profile determined by (3), light velocity in vacuum, and the fiber length, respectively, and k and R are described in (5) and (6), respectively

$$k = \frac{2\pi}{\lambda} \quad (5)$$

$$R = \sqrt{n(r)^2 k^2 - \beta^2 - \frac{\nu^2}{r^2}}. \quad (6)$$

In (6), ν is called the azimuthal mode number. In (4), the poles of r_1 and r_2 in the integrand are defined as the solutions of (7)

$$n(r)^2 k^2 - \beta^2 - \frac{\nu^2}{r^2} = 0 \quad (7)$$

In (4), the wavelength dependence of refractive index (dn/dk) is required as an input parameter. Therefore, in this simulation, the effects of the material and profile dispersions as well as the modal dispersion were taken into account. The material dispersion parameters of the polymers were experimentally measured and inserted into the simulation in the same way as described in [15] and [17].

After calculating the group delay τ of each mode, the time range of the group delay between the fastest and slowest mode was divided into 30 to 40 of time slots. Thus, the impulse response function was constructed by counting the number of modes whose group delay is involved in each time slot. The impulse response function is, in general, calculated by assuming an equal power distribution in all the modes. However, as described in [15], the modal power distribution at the output end of a GI POF is strongly influenced by its differential mode attenuation (DMA). The output waveform was calculated by the convolution of the waveforms of measured input pulse and calculated impulse response function in which the mode power distribution of each POF was accurately estimated by measuring the DMA.

The DMA is important factor influencing the bandwidth performances of the POFs. Therefore, the DMAs of GI and W-shaped POFs were directly measured using a method similar to the NFP measurement mentioned above. Small mode groups were launched via a probe fiber. Then, the attenuation of each mode group was measured by scanning the probe fiber across the input end of the POF. Since the numerical apertures (NAs) of the GI and W-shaped POFs vary in the radial direction according to the refractive index profile, the acceptable light power is the highest at the core center, and gradually decreases from the core center to the periphery. In order to compensate

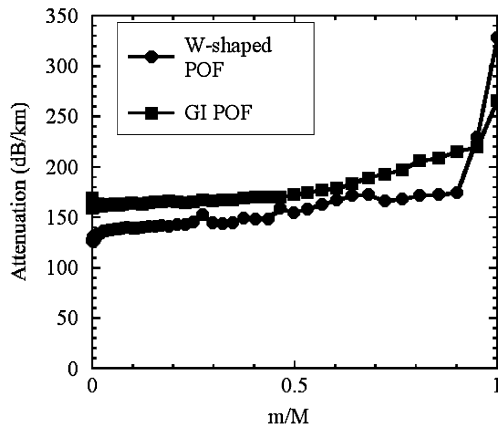


Fig. 7. Comparison of the DMAs in the W-shaped (circle) and the GI (square) POFs at $0.65\text{-}\mu\text{m}$ wavelength.

such a launch power difference, a cut-back method was adopted for DMA measurement. It was already reported that the DMA of MMF would show variable results that were depending on the length of the reference length after the cut-back process [22]. If the reference length after cut-back was too short, the attenuation of high-order modes tended to be high, because excess optical power was still confined in leaky modes in the short length fiber, which would be abruptly eliminated after several tens of meters propagation. Therefore, the appropriate cut-back condition for estimating the DMA of GI POF was investigated, by which the impulse response function was enabled to be accurately simulated.

The measured DMAs of both POFs are shown in Fig. 7. The parameter m in the horizontal axis indicates the principal mode number, and M signifies the maximum m value. In the GI POF, the attenuation of the low-order modes is as low as 150 dB/km , which is comparable to the theoretical limit of the attenuation in the PMMA-based POF [23]. However, the attenuation gradually increases with increasing normalized principal mode number m/M . Therefore, the output pulse broadening from the GI POF was reduced by this high attenuation of high-order modes [15]. It is noteworthy that the attenuation of the intermediate mode group, particularly the modes whose m/M is larger than 0.5 in the W-shaped POF, is lower than that of the GI POF, and an abrupt increment is observed only in the higher order modes whose m/M is larger than 0.9 . From the result of the refractive index profile shown in Fig. 2, the W-shaped POF has a diameter of approximately $500\ \mu\text{m}$, which agrees with the width of the NFP of high-order modes shown in Fig. 4. Therefore, the high-order modes are not attenuated but retain their optical power even after 100-m transmission.

Furthermore, from the result of the DMA in the W-shaped POF, it is found that the total attenuation of the W-shaped POF is as low as that of the conventional GI POF, which means that the formation of the W-shaped index profile showed no influence on the total attenuation of the POF.

Calculated output waveforms from 100-m GI and W-shaped POFs whose index profiles are shown in Fig. 2 are indicated in Fig. 8, where both output pulses with and without DMA consideration are plotted. It is found from Fig. 8 that the output pulses from the W-shaped POF (\bullet, \circ) are calculated to have longer tail part than those from the GI POF (\blacksquare, \square), which is independent of

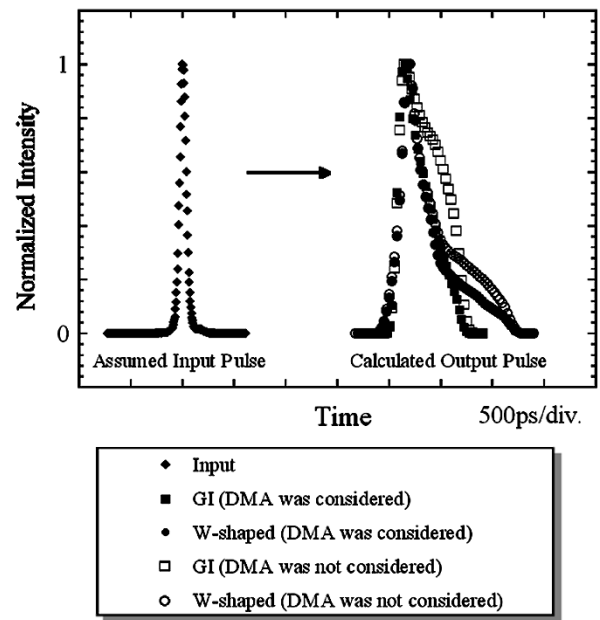


Fig. 8. Calculated output pulse waveforms from the 100-m W-shaped (circles; open: DMA ignored, closed: DMA considered) and GI (square; open: DMA ignored, closed: DMA considered) POFs at $0.65\text{-}\mu\text{m}$ wavelength.

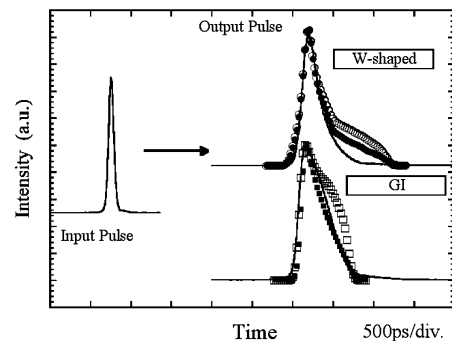


Fig. 9. Measured output pulse waveforms from the 100-m W-shaped and GI POFs compared with the calculated waveforms shown in Fig. 8. Solid line: measured waveform, Plots: calculated waveforms (open circle and square: DMA ignored, closed circle and square: DMA considered).

the DMA consideration. This long tail finally degrades the -3 dB bandwidth. Since the effects of the cladding and the index valley were not considered in these calculations, this difference in the output pulses between the GI and W-shaped POFs particularly when the DMA was not considered attributes to the small difference in the refractive index profile at the quadratic part as shown in Fig. 2. Therefore, it was theoretically confirmed that the bandwidth potential of the GI POF, which was estimated from the quadratic part of refractive index profile was rather slightly higher than that of the W-shaped POF. Furthermore, the DMA of both POFs exhibited a little effect on the pulse broadening as shown in Fig. 8.

In Fig. 9, the experimentally measured waveforms from both POFs are indicated with the calculated waveforms shown in Fig. 8. In the case of the GI POF, although the calculated output waveform when the DMA was not taken into account (\square) is slightly deviated from the measured waveform (solid line), an excellent agreement between the measured and calculated waveforms is observed by considering the measured DMA (\blacksquare).

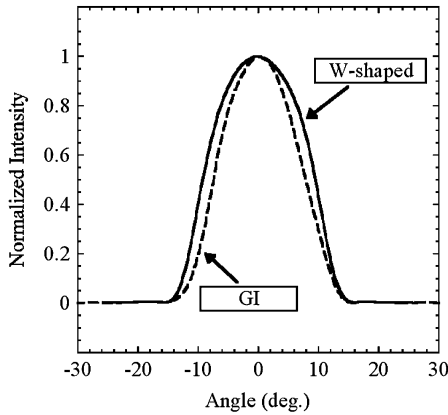


Fig. 10. Measured FFPs from the 100-m W-shaped (solid line) and GI (broken line) POFs.

Thus, the WKB numerical computation process can precisely simulate the output pulse waveform from the GI POF if the experimentally measured DMA was taken into consideration as already mentioned in [15]. On the contrary, a discrepancy is observed and the measured output pulse is rather narrower than that predicted in the W-shaped POF, although the same calculation condition as the GI POF, including the DMA issue was adopted. From the above results, little effect of the DMA on the bandwidth of the W-shaped POF is verified.

Fig. 10 shows the measured far-field patterns (FFP) after 100-m GI and W-shaped POFs transmission, from which the effective NA of the fiber can be estimated. The estimated NAs of the GI and W-shaped POFs from Fig. 10 are 0.201 and 0.222, respectively. The measured NA of the W-shaped POF is slightly higher than that of the GI POF because the high-order modes in the GI POF had high attenuation as shown in Fig. 7. Furthermore, the measured NA of the W-shaped POF is very close to the theoretical value (0.212) calculated from the index profile. The high refractive index of the cladding in the W-shaped POF was a great concern in that the effective numerical aperture might be lowered, which would cause large bending losses compared with that of the GI POF. However, even if the index valley exists at the core cladding boundary, all the modes are well confined in the core region.

The effect of the width of index valley in the W-shaped POF was also studied to confirm the modal dispersion compensation effect of the index valley. A W-shaped POF with an index valley wider than that shown in Fig. 2 was prepared and its bandwidth performance and propagating modal properties were investigated. The measured refractive index profile and the output pulse waveform from a 100-m length are shown in Figs. 11 and 12, respectively. The open circles in Fig. 11 show the approximated curve by power-law form [see (1)] when g was set to be 4.8. The calculated output waveform is also shown in Fig. 12, in which all the dispersions and measured DMA were taken into consideration, while the index valley was not included in the index profile approximation as well. It is noted that the measured output waveform agrees well with the calculated one. Since the index valley is wider than that shown in Fig. 2, the modal dispersion compensation effect by the index valley was decreased, and similar dispersion properties to the normal GI POF were exhibited by the wide-valley W-shaped POF shown in Fig. 11.

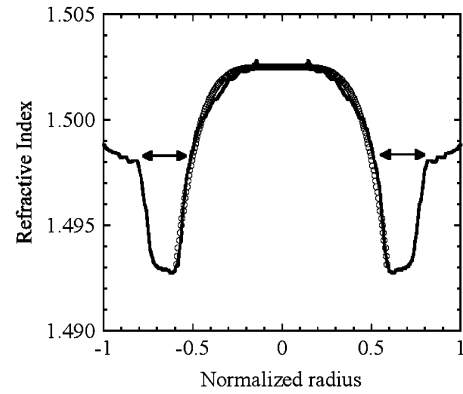


Fig. 11. Refractive index profile of a W-shaped POF with a wide index valley (the width of the valley is shown by arrows). Open Circle: Approximated profile by Power-law form ($g = 4.8$).

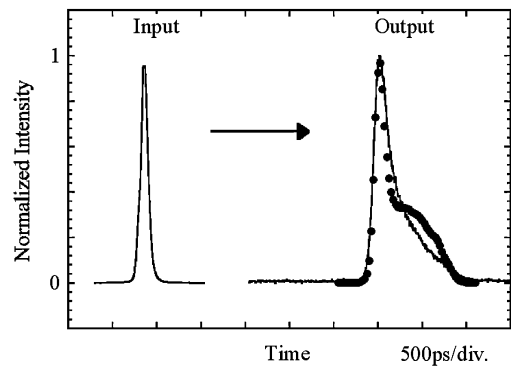


Fig. 12. Measured output pulse waveforms from the 100-m W-shaped POF whose index profile is shown in Fig. 11 compared with the calculated waveforms. Closed circle: Calculated waveform from the index profile shown in Fig. 11 where measured DMA was considered.

Therefore, the steep index valley in the W-shaped POF as shown in Fig. 2 contributed to the disagreement between the measured and calculated waveforms observed in Fig. 9.

D. Differential Mode Delay

Since both index exponents shown in Fig. 2 deviate slightly from the optimum ($g = 2.4$) for the PMMA-based GI POF at $0.65\text{-}\mu\text{m}$ wavelength [17], the delay time difference of each mode can be clearly observed. Therefore, the effect of the valley on the group delay was analyzed by measuring the DMD. The results of both POFs are shown in Fig. 13. In the case of the conventional GI POF, each mode independently propagated having its own delay time, and the high-order modes showed a late arrival compared to the low-order modes (under compensation) as shown in Fig. 13(a). This explicit DMD verified that there was a small mode coupling in the GI POF [15] as mentioned above. The DMD was theoretically calculated by the WKB method [15] from the measured index profile shown in Fig. 2, and the results are plotted in Fig. 13(a) by a broken line. A good agreement is observed between the calculated DMD curve and the measured values shown by the peak position in each pulse [in degrees (\circ)]. Here, the vertical position of each pulse shown in Fig. 13 was adjusted to show that the peak of the pulse (plot) can indicate the group delay of each mode having the normalized principal mode number shown by the vertical axis. The large

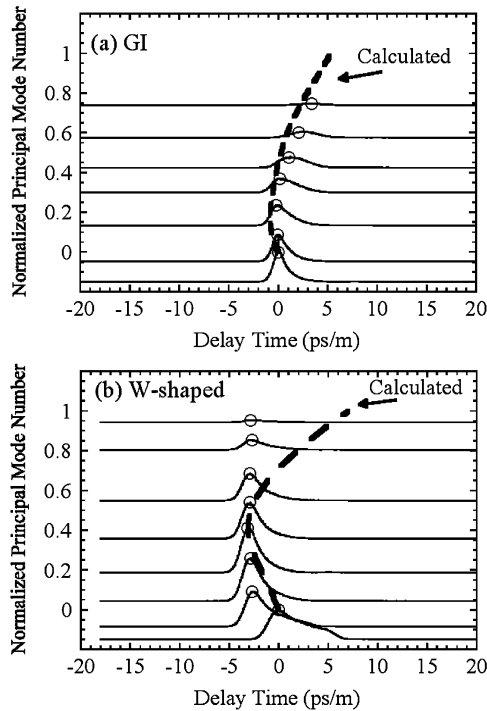


Fig. 13. Measured differential mode delay (DMD) after 100-m transmission through W-shaped and GI POFs at 0.65- μ m wavelength. Broken Line: calculated DMD.

DMD observed in Fig. 13(a) is essentially caused by the modal dispersion in the GI POF.

On the other hand, in the W-shaped POF, each mode also propagated having its own group delay, which means a small mode coupling in the W-shaped POF as well. Although the group delay difference between the highest and lowest order modes is much smaller than that in the GI POF, this delay time contraction is caused not by the mode coupling but by the modal dispersion compensation effect of the refractive index valley. It is noted that the DMD of higher order modes whose normalized principal mode number is larger than 0.9 could be detected in the W-shaped POF as shown in Fig. 13(b), because those modes maintain a sufficiently high optical power for detection even after 100-m transmission. On the contrary, the power of higher order modes (normalized principal mode number >0.8) in the GI POF is attenuated. From these results, it was also verified that the GI POF had high attenuation in the high-order modes compared to that in the W-shaped POF as shown in Fig. 7, and thus, the DMA exhibited less effect on the bandwidth of the W-shaped POF than on that of the GI POF.

The calculated DMD is also plotted in Fig. 13(b) by a broken line in the W-shaped POF. In the DMD calculation for the W-shaped POF, the index valley was neglected as in the approximation for the output waveforms. A large disagreement between the calculated and measured DMD is observed, particularly in the high-order modes. Since the higher order modes carry higher optical power in their evanescent field than the lower order modes, the group delay of the high-order modes is considered to be strongly influenced by the index profile at the core-cladding boundary. It was confirmed that the group delay improvement in the high-order modes in the W-shaped

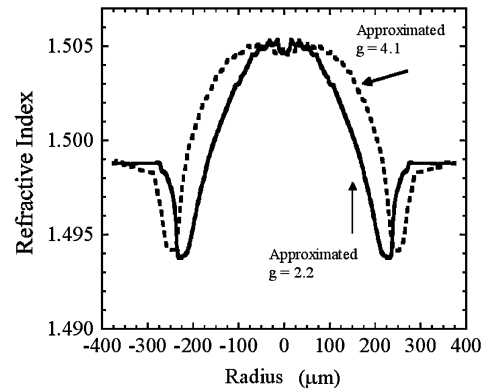


Fig. 14. Representative refractive index profiles of W-shaped POF with different index exponent (g value) in the quadratic part.

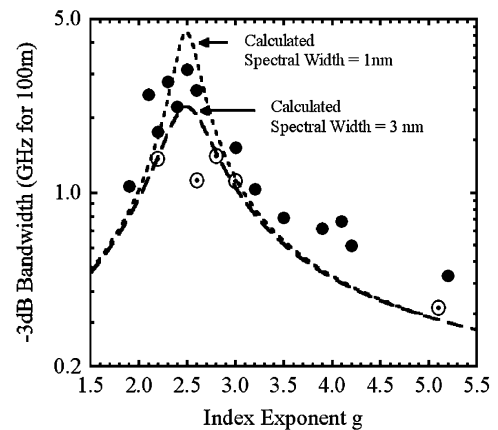


Fig. 15. Relation between the -3 dB Bandwidth at 0.65- μ m wavelength and the index exponent of the W-shaped and GI POFs. Dashed lines are calculated relations, where both modal and material dispersions were considered, while mode coupling was not taken into account.

POF was due to the effect of the index valley. The group delay contraction in high-order modes is considered to be the main reason why the modal dispersion can be decreased by forming the W-shaped index profile in the POF.

E. Variable Refractive Index Exponent

In the previous reports on the W-shaped silica-based MMFs, the dispersion property was calculated by setting the index profile at the quadratic part to be almost ideal such as $g = 2.0$. (In this case, the chromatic dispersion was not concerned [3], [4], [13]). On the other hand, the dispersion improvement was confirmed in the above discussions even if the index exponent g of the quadratic part was slightly larger than its optimum value. ($g_{\text{opt}} = 2.4$) In this paper, the index exponent of the quadratic part in the W-shaped POF was widely varied from $g = 1.7$ to 5.3, (depth ρ was fixed to be almost 2.0) experimentally, then their bandwidth performances were investigated. Representative index profiles are shown in Fig. 14. The bandwidth performances of these W-shaped POFs were measured by the time-domain measurement process under OFL condition as mentioned above, and -3 dB bandwidth was calculated by Fourier Transform of the output and input pulses. Fig. 15 summarizes the relation between the index exponent g and the bandwidth of 100-m PMMA-based GI and W-shaped POFs. Two

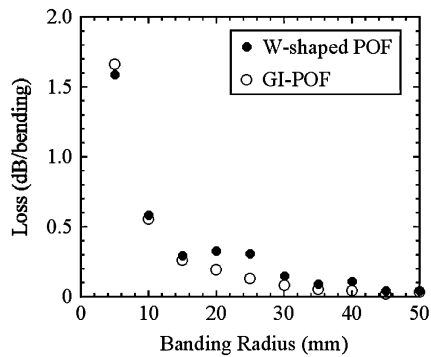


Fig. 16. Comparison of bending losses between W-shaped and GI POFs whose index profiles are shown in Fig. 2. The bending angle was 90° .

dashed lines are calculated relations of GI POF (no-valley) when the spectral widths of light sources were assumed to be 3 nm and 1 nm. Spectral width dependence is clearly observed in the calculated curves when the index exponent closes to the optimum ($g = 2.4$) because the chromatic dispersion becomes dominant in such a fiber with nearly optimum profile. On the contrary, when the index exponent is deviated from optimum, the bandwidth is dominated by the modal dispersion. Plots in Fig. 15 signify the experimentally measured results. In both GI and W-shaped POFs, the samples with small mode coupling were selected. In the case of the conventional GI POF, the measured results (\odot) show almost good agreement with calculated results. On the other hand, the W-shaped POF (\bullet) exhibits higher bandwidth than predicted values for the GI POF in wide g range. These results indicated that the additional modal dispersion compensation effect was provided by the W-shaped profile even when the index profile of the quadratic part is deviated from optimum, compared with the GI POF with uniform index cladding.

F. Bending Loss Properties

From the FFP measurement results described in Section II-C, the W-shaped POF shown in Fig. 2 had the same numerical aperture as that of the GI POF. However, the bending loss would be a concern, because the refractive index of the outermost layer of the W-shaped POF is higher than that of the uniform cladding of the GI POF. Therefore, the bending loss properties of two POFs shown in Fig. 2 were investigated. As the launch condition, the OFL condition was adopted, and the tested fiber was statically bent around a mandrel with a 90° bending angle. The relation between the bending loss and bending radius is shown in Fig. 16. It is found that the bending loss of the W-shaped POF is almost the same as that of the GI POF. Therefore, the NA of the fiber would be the key parameter of the bending loss, and the same NA values between the W-shaped and GI POFs achieved almost the same bending loss values.

IV. CONCLUSION

Modal dispersion compensation in a POF by a W-shaped refractive index profile was demonstrated for the first time. It was theoretically and experimentally confirmed that the effects of mode coupling and DMA were small enough on the higher

bandwidth performance of the W-shaped POF compared with the GI POF. Furthermore, it was also verified that the group delay of higher order modes in the W-shaped POF was strongly influenced by the refractive index valley at the core-cladding boundary. Therefore, we conclude that the index valley in the W-shaped POF plays an important role in increasing the modal bandwidth of the POF.

REFERENCES

- [1] T. Ishigure, E. Nihei, and Y. Koike, "Graded-index polymer optical fiber for high speed data communication," *Appl. Opt.*, vol. 33, pp. 4261–4266, Jul. 1994.
- [2] Y. Koike, T. Ishigure, and E. Nihei, "High-bandwidth graded-index polymer optical fiber," *J. Lightw. Technol.*, vol. 13, pp. 1475–1489, Jul. 1995.
- [3] K. Okamoto and T. Okoshi, "Computer-aided synthesis of the optimum refractive-index profile for a multimode fiber," *IEEE Trans. Microwave Theory Tech.*, vol. 25, pp. 213–221, 1977.
- [4] K. Oyamada and T. Okoshi, "High-accuracy numerical data on propagation characteristics of a-power graded-core fibers," *IEEE Trans. Microwave Theory Tech.*, vol. 28, pp. 1113–1118, 1980.
- [5] P. Pepeljugoski, D. Kuchta, Y. Kwark, P. Pleunis, and G. Kuyt, "15.6-Gb/s transmission over 1 km of next generation multimode fiber," *IEEE Photon. Technol. Lett.*, vol. 14, pp. 717–719, May 2002.
- [6] P. Pepeljugoski, M. J. Hackert, J. S. Abbott, S. E. Swanson, S. E. Golowich, A. J. Ritger, P. Kolesar, Y. C. Chen, and P. Pleunis, "Development of system specification for laser-optimized 50- μ m multimode fiber for multigigabit short-wavelength LANs," *J. Lightw. Technol.*, vol. 21, pp. 1256–1275, May 2003.
- [7] J. B. Schlager, M. J. Hackert, P. Pepeljugoski, and J. Gwinn, "Measurements for enhanced bandwidth performance over 62.5- μ m multimode fiber in short-wavelength local area networks," *J. Lightw. Technol.*, vol. 21, pp. 1276–1285, May 2003.
- [8] P. Pepeljugoski, S. E. Golowich, A. J. Ritger, P. Kolesar, and P. A. Risteski, "Modeling and simulation of next-generation multimode fiber links," *J. Lightw. Technol.*, vol. 21, pp. 1242–1255, May 2003.
- [9] T. Ishigure, Y. Koike, and J. W. Fleming, "Optimum index profile of the perfluorinated polymer based GI polymer optical fiber and its dispersion properties," *J. Lightw. Technol.*, vol. 18, pp. 178–184, Feb. 2000.
- [10] T. Ishigure, A. Horibe, E. Nihei, and Y. Koike, "High-bandwidth, high-numerical aperture graded-index polymer optical fiber," *J. Lightw. Technol.*, vol. 13, pp. 1686–1691, Aug. 1995.
- [11] T. Ishigure, M. Sato, O. Takanashi, E. Nihei, T. Nyu, S. Yamazaki, and Y. Koike, "Formation of the refractive index profile in the graded index polymer optical fiber for gigabit data transmission," *J. Lightw. Technol.*, vol. 15, pp. 2095–2100, Nov. 1997.
- [12] T. Ishigure, S. Tanaka, E. Kobayashi, and Y. Koike, "Accurate refractive index profiling in a graded-index plastic optical fiber exceeding gigabit transmission rates," *J. Lightw. Technol.*, vol. 20, pp. 1449–1556, Aug. 2002.
- [13] T. Okoshi, *Optical Fibers*. New York, NY: Academic Press, Inc., 1982.
- [14] D. G. Cunningham, W. G. Lane, and B. Lane, *Gigabit Ethernet Networking*. Indianapolis, IN: Macmillan, 1999.
- [15] T. Ishigure, M. Kano, and Y. Koike, "Which is a more serious factor to the bandwidth of GI POF: Differential mode attenuation or mode coupling?," *J. Lightw. Technol.*, vol. 18, pp. 959–965, July 2000.
- [16] T. Ishigure, K. Makino, S. Tanaka, and Y. Koike, "High-bandwidth graded-index plastic optical fiber enabling power penalty-free gigabit data transmission," *J. Lightw. Technol.*, vol. 21, pp. 2923–2930, Nov. 2003.
- [17] T. Ishigure, E. Nihei, and Y. Koike, "Optimum refractive index profile of the graded-index polymer optical fiber, toward gigabit data links," *Appl. Opt.*, vol. 35, no. 12, pp. 2048–2053, 1996.
- [18] S. E. Golowich, W. White, W. A. Reed, and E. Knudsen, "Quantitative estimates of mode coupling and differential modal attenuation in perfluorinated graded-index plastic optical fiber," *J. Lightw. Technol.*, vol. 21, pp. 111–121, Jan. 2003.
- [19] *Differential Mode Delay Measurement of Multimode Fiber in the Time Domain*, 2003. TIA-455-220-A.
- [20] W. R. White, M. Dueser, W. A. Reed, and T. Onishi, "Intermodal dispersion and mode coupling in perfluorinated graded-index plastic optical fiber," *IEEE Photon. Technol. Lett.*, vol. 11, pp. 997–999, 1999.
- [21] D. Marcuse, *Principles of Optical Fiber Measurements*. New York, NY: Academic Press, 1981.

- [22] A. R. Mickelson and M. Eriksrud, "Mode-dependent attenuation in optical fibers," *J. Opt. Soc. Amer.*, vol. 73, pp. 1282–1290, Oct. 1983.
- [23] T. Kaino, M. Fujiki, S. Oikawa, and S. Nara, "Low-loss plastic optical fibers," *Appl. Opt.*, vol. 20, pp. 2886–2888, 1981.



Takaaki Ishigure (M'00) was born in Gifu, Japan, on July 30, 1968. He received the B.S. degree in applied chemistry and the M.S. and Ph.D. degrees in material science from Keio University, Japan, in 1991, 1993, and 1996 respectively.

He is currently an Assistant Professor of Keio University. He has been concurrently a group leader of Japan Science and Technology Agency ERATO "Koike Photonics Polymer Project." In 2005, he joined the Department of Electrical Engineering, Columbia University, New York, NY, as a Visiting Research Scientist. His current research interests are in preparation of high-bandwidth graded-index polymer optical fiber and its system design.



Hideki Endo was born in Ibaraki, Japan, on May 20, 1979. He received the B.S. degree in applied physics and physico-informatics and the M.S. degree in integrated design engineering from Keio University, Japan, in 2002 and 2004, respectively.

He is currently with Hitachi, Japan, and his current research interests are in home networking architecture.



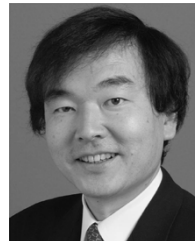
Kunihiko Ohdoko was born in Tokyo, Japan, on October 14, 1979. He received the B.S. degree in applied physics and physico-informatics from Keio University, Japan, in 2003. He is currently working towards the Master's degree in integrated design engineering from Keio University.

His current research interests are in propagating mode analysis in GI and W-shaped POFs.



Keita Takahashi was born in Tokyo, Japan, on August 11, 1981. He received the B.S. degree in applied physics and physico-informatics from Keio University, Japan, in 2004. He is currently working towards the Master's degree in integrated design engineering from Keio University.

His current research interests are in the preparation and characterization of W-shaped POFs.



Yasuhiro Koike (M'02) was born in Nagano, Japan, on April 7, 1954. He received the B.S., M.S., and Ph.D. degrees in applied chemistry from Keio University, Japan, in 1977, 1979, and 1982, respectively.

He has been a Professor of Keio University and developed the high-bandwidth GI polymer optical fiber. He has been concurrently the Director of Japan Science and Technology Agency ERATO "Koike Photonics Polymer Project" since 2000. He stayed as a Visiting Researcher at AT&T Bell Laboratories from 1989 through 1990.

Dr. Koike received the International Engineering and Technology Award of the Society of Plastics Engineers in 1994 and the Fujiwara Award in 2001.